Spectroscopic properties of molecules interacting with small dielectric particles

Joel Gersten

Department of Physics, The City College of the City University of New York, New York, New York 10031

Abraham Nitzan[a)]

Bell Laboratories, Murray Hill, New Jersey 07974
(Received 30 January 1981; accepted 31 March 1981)

Optical properties of small dielectric spheroids with or without adsorbed molecules are studied theoretically. Expressions for the absorption line shapes, the radiative and nonradiative decay rates, and quantum yields are derived. In the case of a molecule near a spheroid the magnitudes differ dramatically from the corresponding case of a molecule near a plane.

I. INTRODUCTION

Recent experimental and theoretical work on surface enhanced Raman scattering (SERS)[1-3] has indicated that at least part, if not all, of the enhancement phenomenon results from the modified local electromagnetic field experienced by the molecule in the vicinity of protrusions on the rough metal substrate. Indeed, SERS has been also reported for molecules adsorbed on metal island films,[2(c),4] colloidal particles,[2(b),5] periodically modulated metal surfaces,[2(h)] and metal particles deposited on posts etched on an inert substrate.[2(d)]

The modified local electromagnetic field which leads to the observed enhancement results from image, shape, and plasmon resonance effects.[3(h)] (The importance of the image effect has been recently challenged by model quantum-mechanical calculations.[6]) It is important to realize that such modification of the local electromagnetic field implies that other optical properties of the adsorbed molecule should also be affected. Indeed, enhanced light absorption[7] and luminescence[8] were recently reported for molecules adsorbed on surface island films, and the possibility of affecting the yields of photochemical reactions on such surfaces was investigated theoretically.[9] We should also keep in mind that these effects are not expected to occur exclusively on rough metal surfaces or on metal particles; some ionic crystals and semiconductors are expected to provide very useful substrate materials in processes involving incident radiation in the red and the infrared.[9]

In this paper we investigate the optical properties of molecules adsorbed on or enclosed in dielectric particles. We focus on properties such as absorption line shapes, lifetime, and quantum yields for emission and for nonradiative energy transfer to the substrate. Our model includes a single spheroidal dielectric particle characterized by its semimajor and semiminor axes a and b, respectively, and by a given dielectric function $\epsilon(\omega)$, and a molecule (represented by a classical point dipole) situated at a given distance R from the particle's center (Fig. 1). Here a, b, and R are assumed to be much smaller than the radiation wavelength. A similar model has been used in our recent study of SERS.[3(h)]

It is important to mention that the same optical properties have been studied both theoretically and experimentally for the case of a molecule adsorbed on a planar, smooth surface.[10] These studies are based on Sommerfeld's treatment of the antenna above a plane problem.[11] An extension of Sommerfeld's work to the antenna above a sphere case has also been given[12]; however, the application to molecular optical properties has not been carried out. As we shall see, the molecular lifetime and the fluorescence yield of the excited molecule depend strongly on the size and shape of the substrate particle.[13]

We should also mention the considerable amount of work associated with Mie scattering of light by small dielectric particles.[14] Of particular interest to our present problem is the recent work by Kerker and coworkers[15] on light scattering by molecules embedded in small particles. While this work addresses mostly properties associated with light scattering experiments (e.g., angular distribution of the scattered radiation), our present work focuses on spectroscopic properties such as lifetimes for radiative or nonradiative rates and yields for fluorescence emission. Furthermore, we are interested mostly in molecules adsorbed outside the dielectric particles, though some problems concerning a molecule embedded inside such particles will also be studied.

This research is aimed at providing a theoretical understanding of recent observations of optical properties of molecules adsorbed on island films or rough

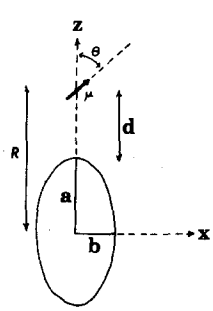

FIG. 1. Geometry of the spheroid–molecule system.

[a)]Present address: Department of Chemistry, Tel Aviv University, Tel Aviv, Israel.

 0021-9606/81/151139-14$01.00

surfaces. In addition to the experiments mentioned above[7,8] it is worthwhile to mention a recent observation of a marked deviation of the observed rate of fluorescence of pyrazine adsorbed on silver from the rate predicted on a smooth planar surface.[16] Our results will also be applicable to molecules interacting with dielectric particles in colloidal solutions or embedded in inert solid matrices. Another potentially useful experimental situation includes molecules adsorbed on or enclosed in clusters formed in supersonic beams.

The present work describes two different approaches to evaluating the optical properties of molecules adsorbed on or embedded in dielectric particles. The first approach, described in Sec. II, evaluates the desired properties by considering appropriate boundary value problems for a system composed of the dielectric particle and the molecular dipole. This approach is particularly suitable for steady state properties. In the second approach (Sec. III) we use an approximation which enables us to derive a set of coupled equations of motion for the molecular dipole and the particle's plasmons. This approach makes it possible to consider transient phenomena. Furthermore, it can be easily generalized to include saturation phenomena and quantum mechanical effects.

In Sec. IV we present numerical results for the optical properties evaluated in Secs. II and III for several interesting models. Finally, in Sec. V we summarize and discuss our results and outline the future direction of this work.[24]

II. SEMICLASSICAL STEADY STATE APPROACH

In this section we describe a semiclassical method for obtaining the radiative and nonradiative decay rates and quantum yield for a system consisting of a small dielectric particle and a molecule. The molecule is taken to be an oscillating point dipole characterized by a dipole moment μ, a polarizability α, and a resonant frequency ω. The dielectric particle is taken to be a spheroid characterized by a size, a shape parameter, and a complex dielectric constant. In all cases of interest it will be assumed that the size of the system is much less than the wavelength of light so that retardation effects may be omitted. This permits the problem to be attacked using an electrostatic approach.

Three problems will be addressed here. First, we consider a spheroid without an additional molecule.[17] Second, we consider a spheroid with a molecule external to it. Finally, we study the case of a molecule inside a spheroidal cavity in a dielectric medium.[18]

Consider an isolated spheroid which has been excited and is oscillating in some electromagnetic mode at frequency ω. For now we may regard this as a steady state oscillation although ultimately we will make use of the correspondence principle and take the energy in the mode to be just $\hbar\omega$. The excited system will have a fluctuating electric dipole moment and this will cause electromagnetic radiation to be produced. This provides the channel for radiative decay. In addition, there can be expected to be fluctuating electric fields throughout the volume of the particle. The Joule heating caused by these fields opens nonradiative decay channels. By computing the power radiated electromagnetically and dividing by the photon energy $\hbar\omega$ we obtain an expression for the radiative decay rate. Likewise, dividing the Joule power by the photon energy gives an expression for the nonradiative decay rate. It is possible to write simple expressions for the decay rates for an arbitrarily shaped small particle in the semiclassical theory:

$$\Gamma_{nr} = \frac{1}{2\hbar\omega} \int \sigma |E|^2 d\mathbf{r} , \tag{II.1}$$

$$\Gamma_r = \frac{\omega^3}{3\hbar C^3} \left| \int \frac{\epsilon - 1}{4\pi} \mathbf{E} d\mathbf{r} \right|^2 , \tag{II.2}$$

where Γ_{nr} is the nonradiative decay rate and Γ_r is the radiative decay rate, σ is the conductivity of the particle, ϵ is its dielectric constant, and $\mathbf{E}$ is the electric field. Note that $\sigma = (\omega/4\pi)\mathrm{Im}\epsilon$. If ϵ is independent of $\mathbf{r}$ within the spheroid, a simple inequality results from applying the Schwartz inequality:

$$\Gamma_r \leq \frac{2\omega^4 V}{3\sigma C^3} \left| \frac{\epsilon - 1}{4\pi} \right|^2 \Gamma_{nr} = \frac{4\pi^2 V}{3\lambda^3} \frac{\Gamma_{nr}}{\mathrm{Im}(\epsilon - 1)^{-1}} , \tag{II.3}$$

where V is the volume of the particle and $\lambda (= 2\pi c/\omega)$ is the wavelength of the radiation field is vacuum. From Eq. (II.3) it is clear that for very small particles the radiative decay rate will be small and so the quantum yield, defined as

$$Y = \frac{\Gamma_r}{\Gamma_r + \Gamma_{nr}} , \tag{II.4}$$

will likewise be small. For particles which are of intermediate size (e.g., $V/\lambda^3 \sim 10^{-3}$), however, Eq. (II.3) does not impose a severe restriction, and relatively high quantum yields may be obtained as we shall see.

Returning to the case of a spheroid, let a be the semimajor axis, b the semiminor axis, and define $f = (a^2 - b^2)^{1/2}$ and $\xi_0 = a/f$. Though the general case may be easily formulated, we shall restrict our attention to the case where the spheroid has been excited in a dipolar mode with the dipole oscillating parallel to the major axis. This restriction is made partly in the interest of simplicity and partly because that mode plays a prominent role in other electromagnetic processes, such as surface enhanced Raman scattering.[3(h)] The resonance frequency of this mode is denoted by ω_1 and is given by

$$[\mathrm{Re}\epsilon(\omega_1)]\, Q_1(\xi_0) = \xi_0 Q_1'(\xi_0) , \tag{II.5}$$

where $Q_1(\xi_0)$ is a Legendre function of the second kind. The radiative and nonradiative decay rates are

$$\Gamma_r = \frac{4}{9} \left(\frac{\omega_1 f}{c} \right)^3 \frac{\xi_0}{(\xi_0^2 - 1)[Q_1(\xi_0)]^2} \mathrm{Re} \left[\frac{\partial \epsilon(\omega_1)}{\partial \omega_1} \right]^{-1} \tag{II.6a}$$

and

$$\Gamma_{nr} = 2\,\mathrm{Im}\epsilon(\omega_1)\,\mathrm{Re} \left[\frac{\partial \epsilon(\omega_1)}{\partial \omega_1} \right]^{-1} . \tag{II.6b}$$

Note that Γ_{nr} is independent of the size of the particle in this limit. Its dependence on shape comes only through the shape dependence of ω_1 [see Eq. (II.5)]. We call the approximation which leads to Eq. (II.6b) the *Drude approximation* for reasons to become clear in Sec. III. Equations (II.4) and (II.6) yield the following expression for the emission yield of the excited spheroid:

$$Y=\left\{1+\frac{9}{2}\left(\frac{C}{\omega_1 f}\right)^3 \mathrm{Im}(\epsilon)\left(\frac{\xi_0^2-1}{\xi_0}\right)[Q_1(\xi_0)]^2\right\}^{-1}. \tag{II.7a}$$

In addition we also derive an expression for the absorption cross section[19] for such a spheroid in an external electromagnetic field. The result is

$$\sigma_a=-\frac{4\pi\omega f^3}{3c}\frac{\xi_0}{(\xi_0^2-1)[Q_1(\xi_0)]^2}\,\mathrm{Im}\left(\frac{1}{\epsilon+\bar{\epsilon}_1}\right), \tag{II.8a}$$

where $\bar{\epsilon}_1=-\xi_0 Q_1'(\xi_0)/Q_1(\xi_0)$.

The corresponding results for a sphere of radius a are obtained by taking the limit $\xi_0\to\infty$ and $f\xi_0\to a$. The nonradiative rate Γ_{nr} remains, of course, as before [Eq. (II.6b)]. The radiative rate, quantum yield, and absorption cross sections become

$$\Gamma_r\to 4\left(\frac{\omega_1 a}{c}\right)^3 \mathrm{Re}\left[\frac{\partial\epsilon(\omega_1)}{\partial\omega_1}\right]^{-1}, \tag{II.6c}$$

$$Y\to\left\{1+\frac{1}{2}\left(\frac{c}{a\omega_1}\right)^3 \mathrm{Im}[\epsilon(\omega_1)]\right\}^{-1}, \tag{II.7b}$$

and

$$\sigma_a\to-\frac{12\pi\omega a^3}{c}\,\mathrm{Im}[\epsilon(\omega)+2]^{-1}. \tag{II.8b}$$

Note that the result (II.8a) is the small sphere limit of the general result by Mie.

From the above expressions it is apparent that the radiative decay rate, the yield, and the absorption cross section are sensitive to both the size (f) and shape (ξ_0) of the spheroid as well as to its dielectric properties.

Next we turn our attention to the case of a molecule near a spheroid. We focus on the case where the molecule is located on a line extending from the major axis and consider both the situation where the dipole is perpendicular ($\perp$) to the surface and where it is parallel ($\parallel$) to it. The decay rates are computed as in the previous problem, but some complications do arise. First of all, in computing the radiative decay rate, one must take into account the total dipole moment of the system and not just the molecular dipole. Secondly, the dipole moment on the molecule is modified by the fact that the local electric field can produce an additional induced dipole. This leads to what may be called an image enhancement factor which turns out to be important only when the molecule is very close to the surface of the spheroid. At such distances the use of classical theory and of idealizing the molecule as a point dipole are somewhat questionable. Evidence from more accurate quantum mechanical calculations[6] indicates that this factor is considerably suppressed.

Let d denote the distance of the molecule from the apex of the spheroid and $\xi_1=(a+d)/f$. The radiative decay rate is obtained to be for the $\perp$ orientation

$$\Gamma_r(\perp)=\frac{\omega^3|\mu_0|^2}{3\hbar C^3|1-\Delta(\perp)|^2}\left|1+\frac{1-\epsilon}{\epsilon+\bar{\epsilon}_1}\frac{\xi_0 Q_1'(\xi_1)}{Q_1(\xi_0)}\right|^2, \tag{II.9}$$

and for $\parallel$ orientations

$$\Gamma_r(\parallel)=\frac{\omega^3|\mu_0|^2}{3\hbar C^3|1-\Delta(\parallel)|^2}\left|1+\frac{1-\epsilon}{\epsilon+\bar{\epsilon}_1^{(1)}}\frac{P_1^{(1)}(\xi_0)Q_1^{(1)}(\xi_1)}{(\xi_1^2-1)^{\frac{1}{2}}Q_1^{(1)}(\xi_0)}\right|^2, \tag{II.10}$$

where

$$\Delta(\perp)=\alpha f^{-3}\sum(2n+1)(\epsilon-1)P_n(\xi_0)[Q_n'(\xi_1)]^2[(\epsilon+\bar{\epsilon}_n)Q_n(\xi_0)]^{-1}$$

and

$$\Delta(\parallel)=\alpha(2f)^{-3}\sum(2n+1)(1-\epsilon)P_n'(\xi_0)\times[Q_n'(\xi_1)]^2[(\epsilon+\bar{\epsilon}_n^{(1)})Q_n'(\xi_0)]^{-1}.$$

In Eq. (II.10) $P_1^{(1)}$ and $Q_1^{(1)}$ denote associated Legendre functions of the first and second kind, respectively. The transition moment of the bare molecule has been denoted by μ_0. The quantities $\bar{\epsilon}_1$ and $\bar{\epsilon}_1^{(1)}$ appearing above are defined by

$$\bar{\epsilon}_n=-\frac{P_n(\xi_0)Q_n'(\xi_0)}{Q_n(\xi_0)P_n'(\xi_0)} \tag{II.11}$$

and

$$\bar{\epsilon}_n^{(1)}=-\frac{P_n^{(1)}(\xi_0)Q_n^{(1)\prime}(\xi_0)}{P_n^{(1)\prime}(\xi_0)Q_n^{(1)}(\xi_0)}. \tag{II.12}$$

The nonradiative decay rates due to energy transfer to the spheroid are

$$\Gamma_{nr}(\perp)=-\frac{|\mu_0|^2}{2\hbar f^3(\xi_0^2-1)|1-\Delta(\perp)|^2}\times\sum_n(2n+1)\,\mathrm{Im}\left(\frac{1}{\epsilon+\bar{\epsilon}_n}\right)\frac{P_n(\xi_0)}{P_n'(\xi_0)}\left[\frac{Q_n'(\xi_1)}{Q_n(\xi_0)}\right]^2, \tag{II.13}$$

and

$$\Gamma_{nr}(\parallel)=-\frac{|\mu_0|^2}{4\hbar f^3(\xi_0^2-1)(\xi_1^2-1)|1-\Delta(\parallel)|^2}\times\sum_n n(n+1)(2n+1)\,\mathrm{Im}\left(\frac{1}{\epsilon+\bar{\epsilon}_n^{(1)}}\right)\frac{P_n^{(1)}(\xi_0)}{P_n^{(1)\prime}(\xi_0)}\times\left[\frac{Q_n^{(1)}(\xi_1)}{Q_n^{(1)}(\xi_0)}\right]^2. \tag{II.14}$$

Expressions for Eqs. (II.9), (II.10), (II.13), and (II.14) in the limit where the spheroid degenerates to a sphere are readily obtained.[24] If the molecule is sufficiently close to the sphere that it may be thought of as a plane, these equations simplify further.[24] From the above equations it is again obvious that the decay rates depend, in a nontrivial way, on the size and shape of the particle as well as on the distance of the molecule from the particle and their relative orientation. As we show below (Sec. IV), these effects are substantial.

Our final problem consists of studying a molecule inside in a spheroidal cavity. Even though this problem is not directly related to the others considered in this

paper, we include it here because the radiative lifetime of such a molecule can be easily evaluated by using the methods employed here. The resulting expression for the radiative decay rate may be used as a model for the radiative behavior of a molecule in a dielectric medium.

The molecule is positioned along the major axis with its dipole parallel to the axis. The medium outside the cavity is allowed to have a complex dielectric constant ϵ_0 while the medium inside the cavity has a real dielectric constant ϵ_1. We must restrict our attention to real ϵ_1 in order to have a finite amount of Joule heating. A problem of interpretation arises in the case where ϵ_0 is complex. Strictly speaking, we cannot have radiation at infinity if the outer medium is absorbing. One must then regard the radiation as a mechanism for producing long range energy deposition whereas the nonradiative processes produce short range energy deposition.

Local fields can again induce additional dipole moments on the molecule. We find the following expression for the radiative decay rate:

$$\Gamma_{nr} = -\frac{|\mu_0|^2}{2\hbar f^3(\xi_0^2-1)|1-\Delta|^2}\sum_n \frac{(2n+1)[P_n'(\varphi_1)]^2}{P_n(\xi_0)P_n'(\xi_0)} \times \mathrm{Im}\left(\frac{1}{\epsilon_1+\epsilon_0\epsilon_n}\right), \tag{II.15}$$

where

$$\Delta = -\alpha\sum(2n+1)(\epsilon_0-\epsilon_1)P_n(\varphi_1)P_n'(\varphi_1)Q_n'(\xi_0) \times[\epsilon_0\epsilon_1 f^3 P_n'(\xi_0)(\bar{\epsilon}_1+\epsilon_1/\epsilon_0)]^{-1}$$

and $\varphi_1=\xi_1$ or η_1, depending on whether $|Z|>f$ or $|Z|<f$. The radiative decay rate is given by

$$\Gamma_r = \frac{\omega^3|\epsilon_0|^{1/2}|\mu_0|^2}{3\hbar C^3(\xi_0^2-1)^2[Q_1(\xi_0)]^2|1-\Delta|^2}\left|\frac{1}{\bar{\epsilon}_1+\epsilon_1/\epsilon_0}\right|^2. \tag{II.16}$$

The nonradiative rate is a complicated function of the shape of the cavity. To the extent that the factor Δ may be neglected in Eq. (II.16), the radiative rate is independent of both the size of the cavity and the molecule's location along the axis.

Note that the dependence of Γ_r on ϵ_0 is different from what is obtained for a molecule embedded in a continuous dielectric medium ($\Gamma_r \sim \sqrt{\epsilon_0}$). It should be interesting to compare these results to the actual observed radiative behavior of molecules in dielectric media.

III. TIME DEPENDENT APPROACH

The calculations described in Sec. II are useful for the evaluation of many optical properties of molecules interacting with small dielectric particles. In this section we describe an alternative approach which considers the system as composed of the molecular dipole and the particle's plasmons and provides the Hamiltonian and the equations of motion for this system in the presence of the incident radiation field. Even though this is achieved at the price of additional approximations, the result is highly useful because it enables us to consider the nonstationary processes and is also easily extended to quantum mechanical systems. This approach has been recently used to consider the feasibility of enhancing photochemical reactions on rough surfaces.[9]

In what follows we shall limit ourselves to the case of a molecule (polarizable point dipole) lying outside (a distance R from the center of) a small dielectric sphere of radium a ($a<R$) and dielectric function $\epsilon(\omega)=\epsilon_1(\omega)+i\epsilon_2(\omega)$. All distances are taken to be much smaller than the wavelength of light.

Our procedure relies on a model of an "ideal particle" which is defined as a particle for which each plasmon resonance is associated with an independent harmonic plasmon mode. For a sphere this implies the sphere plasmon Hamiltonian

$$H_s = \sum_{l=0}^{\infty}\sum_{m=-l}^{l}\hbar\omega_l b_{lm}^* b_{lm}, \tag{III.1}$$

and the equations of motion for the plasmon amplitudes b_{lm} b_{lm}^* are

$$\dot{b}_{lm} = -\frac{i}{\hbar}\frac{\partial H_s}{\partial b_{lm}^*}, \quad \dot{b}_{lm}^* = \frac{i}{\hbar}\frac{\partial H_s}{\partial b_{lm}}, \tag{III.2}$$

where ω_l are the plasmon resonance frequencies and $\hbar$ is the Planck constant. We have deliberately chosen a representation which may be straightforwardly quantized.

The amplitude b_{lm} and its complex conjugate b_{lm}^* represent the degree of excitation of the l, m plasmon. Their physical significance is shown from the following result for the (uncharged) sphere potential

$$\phi_s(r,\theta,\phi) = \sum_{l=1}^{\infty}\sum_{m=-l}^{l}[G_{lm}(r,\theta,\phi)b_{lm} + G_{lm}^*(r,\theta,\phi)b_{lm}^*], \tag{III.3}$$

where (r,θ,ϕ) is the point where the potential is measured relative to the sphere center as an origin and where

$$G_{lm}(r,\theta,\phi) = \left[\frac{4\pi\hbar}{al\epsilon_1'(\omega_l)}\right]^{1/2} Y_{lm}(\theta,\phi)\begin{cases}(r/a)^{-l-1}, & r>a,\\ (r/a)^l, & r<a.\end{cases} \tag{III.4}$$

If a point dipole μ is located on the z axis at a point $r=R$, $\theta=\varphi=0$ outside the sphere, the Hamiltonian contains a term corresponding to the sphere–dipole interaction. This is

$$H_{sd} = -\mu\cdot\mathbf{E}_s = \mu\cdot\nabla\phi_s = \mu_x\left(\frac{\partial\phi_s}{\partial r}\right)_{R,0,0} + \frac{\mu_z}{R}\left(\frac{\partial\phi_s}{\partial\theta}\right)_{R,0,0}, \tag{III.5}$$

where we have taken the dipole to lie in the zx plane, μ_x and μ_z being its components in the x and z directions, respectively. Using Eqs. (III.3)–(III.5) together with some elementary properties of spherical harmonics, we obtain

$$H_{sd} = -\mu_z \sum_l \left[\frac{\hbar(2l+1)(l+1)^2}{a^3 l\, \epsilon_1'(\omega_l)}\right]^{1/2} \left(\frac{a}{R}\right)^{l+2} (b_{l0} + b_{l0}^*) - \mu_x \sum_l \left[\frac{\hbar(2l+1)(l+1)}{4a^3 \epsilon_1'(\omega_l)}\right]^{1/2} (b_{l1} - b_{l,-1} + b_{l1}^* - b_{l,-1}^*) \times \left(\frac{a}{R}\right)^{l+2} . \quad \text{(III.6)}$$

The Hamiltonian also contains a term describing the interaction between the sphere and the external (homogeneous in our limit) radiation field. This is given by

$$H_{sE} = -\mu_s \cdot \mathbf{E} = -\mu_{sx} E_x - \mu_{sy} E_y - \mu_{sz} E_z , \quad \text{(III.7)}$$

where E_x, E_y, and E_z are the components of the electric field amplitude and where μ_s is the dipole moment of the dielectric sphere. The latter may be obtained in terms of the plasmon amplitudes by comparing the potential of the far field of the sphere inferred from Eqs. (III.3) and (III.4) with the potential associated with a point dipole $\varphi(r, \theta, \phi) = (\mu_{sz}\cos\theta + \mu_{sx}\sin\theta\cos\phi + \mu_{sy}\sin\theta\sin\phi)/r^2$. We get

$$\mu_{sz} = K(b_{10} + b_{10}^*) ,$$
$$\mu_{sx} = -\frac{K}{\sqrt{2}} (b_{11} + b_{11}^* - b_{1,-1} - b_{1,-1}^*) , \quad \text{(III.8)}$$
$$\mu_{sy} = -\frac{iK}{\sqrt{2}} (b_{11} - b_{1,1}^* + b_{1,-1} - b_{1,-1}^*) ,$$

where

$$K = \left[\frac{3\hbar a^3}{\epsilon_1'(\omega_1)}\right]^{1/2} . \quad \text{(III.9)}$$

ω_1 is the dipolar plasmon resonance frequency [$\epsilon_1(\omega_1) = -2$]. Inserting Eq. (III.8) into Eq. (III.7), we get the final form of the sphere–radiation field interaction Hamiltonian

$$H_{sE} = K\left[-E_z b_{10} + \frac{1}{\sqrt{2}} (E_x + iE_y) b_{11} - \frac{1}{\sqrt{2}} (E_x - iE_y) b_{1,-1} + \text{c.c.}\right] , \quad \text{(III.10)}$$

where c.c. denotes complex conjugate.

The Hamiltonian terms derived so far have to be supplemented by the Hamiltonian of the molecule which is modeled as an oscillating dipole μ which is a function of an intramolecular coordinate ρ:

$$H_d = \frac{m}{2} [\dot{\rho}^2] + V(\rho) , \quad \text{(III.11)}$$

where m is the associated mass and $V(\rho)$ is the corresponding potential. We also need to know the relation between μ and ρ:

$$\mu = \mu(\rho) . \quad \text{(III.12)}$$

Finally, the interaction between the molecular dipole and the incident radiation field is given by

$$H_{dE} = -\mu(\rho) \cdot \mathbf{E} . \quad \text{(III.13)}$$

With this we have completed the derivation of the Hamiltonian for the molecule–sphere system in the presence of the incident radiation field. It is given by

$$H = H_s + H_d + H_{sd} + H_{sE} + H_{dE} , \quad \text{(III.14)}$$

where the different contributions to the rhs are given by Eqs. (III.1), (III.11), (III.6), (III.10), and (III.13).

The equations of motion for the plasmon amplitudes and for the molecular dipole are obtained from

$$\dot{b}_{lm} = -\frac{i}{\hbar} \frac{\partial H}{\partial b_{lm}^*} - \frac{\gamma_l}{2} b_{lm} , \quad \text{(III.15a)}$$

$$\dot{b}_{lm}^* = \frac{i}{\hbar} \frac{\partial H}{\partial b_{lm}} - \frac{\gamma_l}{2} b_{lm} , \quad \text{(III.15b)}$$

and

$$\ddot{\rho} + \frac{1}{m} \frac{\partial V(\rho)}{\partial \rho} + \Gamma^{(f)} \dot{\rho} = -\frac{1}{m} \frac{\partial}{\partial \rho} (H_{sd} + H_{dE}) , \quad \text{(III.16)}$$

where we have introduced phenomenological terms corresponding to damping of the plasmons and the molecular motion. γ_l is given by

$$\gamma_l = 2 \frac{\epsilon_2(\omega_l)}{\epsilon_1'(\omega_l)} , \quad \text{(III.17)}$$

and $\Gamma^{(f)} = \Gamma_r^{(f)} + \Gamma_{nr}^{(f)}$ is the total decay rate (radiative and nonradiative) associated with the free molecule. Note that $\gamma_1 = \Gamma_{nr}^{(s)}$, where $\Gamma_{nr}^{(s)}$ is defined by Eq. (II.6b).[20] The derivative with respect to ρ in Eq. (III.16) is taken using a given functional form $\mu(\rho)$ [Eq. (III.12)].

The system of equations (III.12)–(III.15) can be simplified if (as is usually the case) the $l>1$ plasmon modes are not coupled to the radiation field; their only way to be excited is by energy transfer from the molecule. Also, since γ_l are quite large (see Table I, the b_{lm} ($l>1$) amplitudes remain small, and back transfer of energy from these modes to the molecule is negligible. Under these circumstances we disregard the $l>1$ modes and represent their effect on the molecular motion as a dissipation channel, replacing $\Gamma^{(f)}$ by

$$\Gamma = \Gamma^{(f)} + \Gamma_{nr,s}' . \quad \text{(III.18)}$$

$\Gamma_{nr,s}'$ is the additional decay rate of the molecule due to its coupling with the $l>1$ sphere plasmons.[21] It depends on the molecular orientation relative to the sphere. If θ is the angle between the molecular dipole and the z (sphere center–molecule) axis and if $\Gamma_{nr,s}'(\perp)$ and $\Gamma_{nr,s}'(\parallel)$ correspond to $\theta = 0$ and $\theta = \pi/2$, respectively, we have

$$\Gamma_{nr,s}' = \Gamma_{nr,s}'(\perp)\cos^2\theta + \Gamma_{nr,s}'(\parallel)\sin^2\theta . \quad \text{(III.19)}$$

There is also a corresponding frequency shift which can be usually neglected in cases where the present classical theory is valid.

Under these conditions the equation for the molecular motion becomes

$$\ddot{\rho} + \frac{1}{m} \frac{\partial V(\rho)}{\partial \rho} + \Gamma \dot{\rho} = \frac{1}{m} \left[\frac{\partial \mu_z}{\partial \rho} \left(\frac{2\sqrt{2}}{R^3} K\beta_0 + E_z\right) + \frac{\partial \mu_x}{\partial \rho} \left(\frac{1}{R^3} K\beta_1 + E_x\right)\right] , \quad \text{(III.20)}$$

where

$$\beta_0 = \frac{1}{\sqrt{2}} (b_{10} + b_{10}^*) \quad \text{(III.21a)}$$

TABLE I. Some characteristic numbers for silver, gold, and copper particles. ω_1 is the resonance frequency of the dipolar sphere (or spheroid in the direction of the long axis) plasmon; ω_2 is the resonance frequency of the $l=2$ sphere plasmon; $\Gamma^s_{nr}(=\gamma_1)$ is the radiationless damping rate of the dipolar plasmon; γ_2 is the same for the $l=2$ plasmon; Γ^s_r is the radiative decay rate of the dipolar plasmon; $\Gamma^{\perp}_{nr,s}$ and $\Gamma^{\perp}_{r,s}$ are the nonradiative (due to energy transfer to the particle) and radiative lifetime of an excited molecule, respectively, in the normal configuration a given distance (8 Å here) from the particle surface. In the case of a spheroid the molecule is placed along the long axis. The spheroid is characterized by an aspect ratio $a/b=1.75$.

	ω_1 (cm^{-1})	ω_2 (cm^{-1})	$\Gamma^s_{nr}=\gamma_1$ (cm^{-1})	γ_2 (cm^{-1})	Γ^s_r (cm^{-1})	$\Gamma^{\perp}_{nr,s}$ (8 Å) (cm^{-1})	$\Gamma^{\perp}_{r,s}$ (8 Å) (cm^{-1})
Ag (sphere)	28 230	28 890	761	904	239	22.4	0.081
Ag (spheroid)	25 500	···	504	···	721	35.6	14.2
Au (sphere)	20 690	26 700	15 910	52 950	129	161.0	0.022
Au (spheroid)	18 900	···	2313	···	107		
Cu (sphere)	27 300	30 250	44 030	53 680	664	155	0.024
Cu (spheroid)	22 700	···	23 130	···	773		

and

$$\beta_1 = \frac{1}{\sqrt{2}}\,(b_{11}+b^*_{11}-b_{1,-1}-b^*_{1,-1})\ . \tag{III.21b}$$

Equations (III.15a) and (III.15b) for the motion of the $l=1$ modes may be combined to give

$$\ddot{\beta}_0+\left(\omega_1^2+\frac{\gamma_1^2}{4}\right)\beta_0+\gamma_1\dot{\beta}_0=\frac{\sqrt{2}K}{\hbar}\,\omega_1\left(\frac{2}{R^3}\ \mu_z+E_z\right), \tag{III.22a}$$

$$\ddot{\beta}_1+\left(\omega_1^2+\frac{\gamma_1^2}{4}\right)\beta_1+\gamma_1\dot{\beta}_1=\frac{2K}{\hbar}\,\omega_1\left(\frac{1}{R^3}\ \mu_x-E_x\right). \tag{III.22b}$$

Equations (III.20) and (III.22) together with Eqs. (III.12) and (III.17)–(III.19) constitute our final set of equations for the coupled motions of the molecular dipole and the dipolar modes of the sphere in the presence of the incident radiation field (represented by its time dependent electric field components). The following points should be noted:

(a) A more transparent form for these equations is obtained by making use of Eqs. (III.8) in the form

$$\mu_{sz}=\sqrt{2}K\beta_0\ ,\quad \mu_{sx}=-K\beta_1\ . \tag{III.23}$$

Using also Eq. (III.9), we get

$$\ddot{\rho}+\frac{1}{m}\ \frac{\partial V(\rho)}{\partial\rho}+\Gamma\dot{\rho}=\frac{1}{m}\left[\frac{\partial\mu_z}{\partial\rho}\left(\frac{2}{R^3}\ \mu_{sz}+E_z\right)+\frac{\partial\mu_x}{\partial\rho}\left(-\frac{1}{R^3}\ \mu_{sx}+E_x\right)\right], \tag{III.24}$$

$$\ddot{\mu}_{sz}+\left(\omega_1^2+\frac{\gamma_1^2}{4}\right)\mu_{sz}+\gamma_1\dot{\mu}_{sz}=\omega_1^2\,\alpha_s\left(\frac{2}{R^3}\ \mu_z+E_z\right), \tag{III.25}$$

$$\ddot{\mu}_{sx}+\left(\omega_1^2+\frac{\gamma_1^2}{4}\right)\mu_{sx}+\gamma_1\dot{\mu}_{sx}=\omega_1^2\,\alpha_s\left(-\frac{1}{R^3}\,\mu_x+E_x\right), \tag{III.26}$$

where

$$\alpha_s=\frac{6a^3}{\omega_1\epsilon_1'(\omega_1)}\ . \tag{III.27}$$

In Eqs. (III.24)–(III.26) the dipolar sphere plasmons appear as Drude oscillators located at the center of the sphere and characterized by the resonance frequency ω_1 [$\epsilon(\omega_1)=-2$], damping rate γ_1 [Eq. (III.17)], and by a static polarizability α_s.

(b) The apparent static polarizability α_s [Eq. (III.27)] of the sphere should not be confused with the true static polarizability given by $\{[\epsilon(0)-1]/[\epsilon(0)+2]\}a^3$. α_s is the polarizability which appears in the Drude approximation [Eqs. (III.25) and (III.26)] for the motion of the dipolar sphere plasmons in the vicinity of $\omega=\omega_1$.

(c) The form (III.24) of the molecular equation is useful when multiphoton excitation of the nuclear motion is considered.[9] In the case of a weak field excitation of a two level system (e.g., electronic transition in atoms) the harmonic limit of Eq. (III.24) is valid. Putting $V(\rho)=\frac{1}{2}m\omega^2\rho^2$, $\partial\mu_z/\partial\rho=e\cos\theta$, and $\partial\mu_x/\partial\rho=e\sin\theta$, and introducing the radiative decay rate of the free molecule in vacuum

$$\Gamma_r^{(f)}=\frac{2}{3}\ \frac{e^2}{m\omega}\left(\frac{\omega}{c}\right)^3, \tag{III.28}$$

we may rewrite Eq. (III.24) in the form

$$\ddot{\mu}+\omega^2\mu+\Gamma\dot{\mu}=\omega^2\alpha\left[\left(\frac{2}{R^3}\ \mu_{sz}+E_z\right)\cos\theta+\left(-\frac{1}{R^3}\ \mu_{sx}+E_x\right)\sin\theta\right], \tag{III.29}$$

where

$$\alpha=\frac{3}{2}\ \frac{\Gamma_r^{(f)}}{\omega}\left(\frac{c}{\omega}\right)^3\ . \tag{III.30}$$

In this form the molecule is represented as a Drude oscillator characterized by a frequency ω, damping $\Gamma(\theta)$, and polarizability α.

We end this section by considering some simple applications of the time dependent formalism. More applications are described in Ref. 9.

A. Absorption line shape by a sphere

The Drude equation for the sphere dipolar plasmon in the absence of a molecule

$$\ddot{\mu}_s + \left(\omega_1^2 + \frac{\gamma_1^2}{4}\right)\mu_s + \gamma_1 \dot{\mu}_s = \omega_1^2 \alpha_s E \qquad \text{(III.31)}$$

implies[9] the following absorption cross section:

$$\sigma_a(\omega) = \frac{\pi \alpha_s}{c}\left(\omega_1^2 + \frac{\gamma_1^2}{4}\right)\frac{\gamma_1}{(\omega_1-\omega)^2 + \frac{\gamma_1^2}{4}} . \qquad \text{(III.32)}$$

This can be compared to the exact result [Eq. (II.8b)] as a check on the quality of the Drude approximation for the motion of the sphere plasmon. We present this comparison in Sec. IV.

B. Radiative lifetime of the sphere

As Eq. (III.31) indicates, the sphere dipolar plasmon behaves in the Drude approximation as a dipole of polarizability α_s. Equation (III.30) then implies that its radiative decay rate is (assuming $\gamma_1 \ll \omega_1$)

$$\Gamma_r^{(s)} = \tfrac{2}{3}\omega_1\left(\frac{\omega_1}{c}\right)^3 \alpha_s , \qquad \text{(III.33)}$$

and using Eq. (III.27) we get

$$\Gamma_r^{(s)} = \frac{4}{\epsilon_1'(\omega_1)}\left(\frac{\omega_1 a}{c}\right)^3 , \qquad \text{(III.34)}$$

in agreement with Eq. (II.6c), which was obtained in the steady state approach.

C. The apparent yield

The expressions for the emission yield of an excited molecule near a dielectric spheroid [$\Gamma_r/(\Gamma_r+\Gamma_{nr})$, where Γ_r and Γ_{nr} are given by Eqs. (II.9) and (II.10) or (II.13) and (II.14), respectively] are rarely measured for adsorbed molecules. More often the emission intensity is monitored for a fixed incident intensity while some characteristics of the system (e.g., molecule–surface distance or surface structure) are varied.[8] This observed emission intensity is not normalized by the energy adsorbed and we therefore call it the apparent quantum yield. In what follows we calculate the apparent quantum yield for the case of a molecule near a sphere in the normal configuration. Let ω_0 be the incident frequency, ω_a the molecular resonance frequency in absorption, and ω_b the molecular emission frequency. The dipole induced on the molecule is given by

$$\mu = \frac{\alpha E_{\rm loc}}{\omega_a^2 - \omega_0^2 - i\omega_0\Gamma} , \qquad \text{(III.35)}$$

where $E_{\rm loc}$ is the local electric field amplitude. If the local field resulting from the molecule image is disregarded, we have

$$E_{\rm loc} = \left[1 + 2\,\frac{\epsilon(\omega_0)-1}{\epsilon(\omega_0)+2}\left(\frac{a}{R}\right)^3\right]E_{\rm inc} . \qquad \text{(III.36)}$$

Here the incident field amplitude $E_{\rm inc}$ as well as $E_{\rm loc}$ refer to the corresponding z components. To evaluate the emission intensity, the dipole amplitude in Eq. (III.35) is taken to oscillate with frequency ω_b. The total dipole of this frequency induced in the system is

$$\mu_{\rm tot} = \left[1 + 2\,\frac{\epsilon(\omega_b)-1}{\epsilon(\omega_b)+2}\left(\frac{a}{R}\right)^3\right]\mu . \qquad \text{(III.37)}$$

The emission intensity is proportional to $|\mu_{\rm tot}|^2$. We get

$$Y_{\rm app} = \left|1 + 2\,\frac{\epsilon(\omega_b)-1}{\epsilon(\omega_b)+1}\left(\frac{a}{R}\right)^3\right|^2\left|1 + 2\,\frac{\epsilon(\omega_a)-1}{\epsilon(\omega_a)+2}\left(\frac{a}{R}\right)^3\right|^2 \times \frac{(\omega_a^2-\omega_0^2)^2 + \omega_0^2\Gamma^{(f)2}}{(\omega_a^2-\omega_0^2)^2 + \omega_0^2\Gamma^2} , \qquad \text{(III.38)}$$

or, for $\omega_0 = \omega_a$,

$$Y_{\rm app} = \left|\left[1 + 2\,\frac{\epsilon(\omega_b)-1}{\epsilon(\omega_b)+2}\left(\frac{a}{R}\right)^3\right]\times\left[1 + 2\,\frac{\epsilon(\omega_a)-1}{\epsilon(\omega_a)+2}\left(\frac{a}{R}\right)^3\right]\right|^2\left(\frac{\Gamma^{(f)}}{\Gamma}\right)^2 , \qquad \text{(III.39)}$$

where we have normalized $Y_{\rm app}$ to be unity for the free molecule. The extension of this result to nonnormal configurations and for a spheroidal substrate is straightforward.

IV. RESULTS AND DISCUSSION

In Sec. II we have studied three problems involving a spheroidally shaped dielectric particle and expressions for the radiative and nonradiative cross sections and quantum yields have been derived. The three problems of interest consisted of an isolated spheroid, a molecule near a spheroid, and a molecule inside a spheroidal cavity. In addition, formulas were obtained for the limit where the spheroid degenerates to a sphere. The validity of the formalism used has been verified by performing similar calculations for a molecule near a plane surface and comparing the results to those available in the literature.[10] For the small sphere case we also derived in Sec. III approximate equations of motion for the molecule–plasmon system. Aside from the intrinsic interest in the behavior of small particles, spheroids are of interest because they model, in a crude way, the surface roughness features of moderately rough surfaces. Thus, the formulas derived have some validity when discussing the optical properties of rough dielectric (or metal) surfaces with or without adsorbed molecules.

Let us start by presenting some results pertaining to the isolated spheroid. Our result for the radiationless decay rate of the isolated spheroid stems from what we called the Drude approximation, which essentially consists of viewing each plasmon mode as an independent damped harmonic oscillator, with a frequency independent damping coefficient. For our procedure to be valid, the particle's plasmons have to be well separated in frequency relative to their damping width [in addition to the requirement that[20] $\epsilon_2'(\omega_r) \ll \epsilon_1'(\omega_r)$]. Table I shows that for the $l=1$, 2 plasmons this is satisfied reasonably well for silver, only very roughly for gold, and not at all for copper. In Fig. 2 we compare the absorption line shapes calculated for spheres of silver and copper using the exact expression and the Breit–Wigner form. We see that for Ag the approximation is good, while it fails for Cu. Obviously, for higher l plasmons the overlap is large and they can no longer be viewed as independent oscillators in any real dielectric.

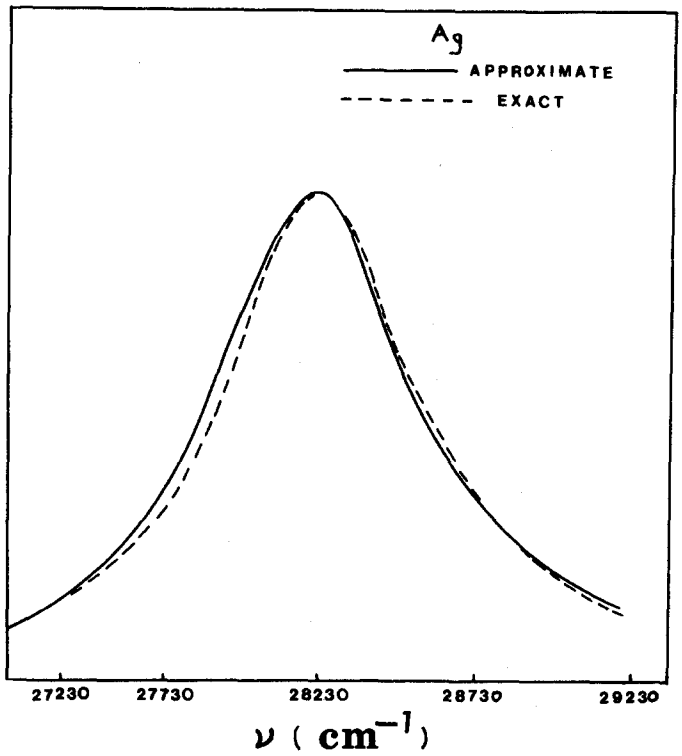

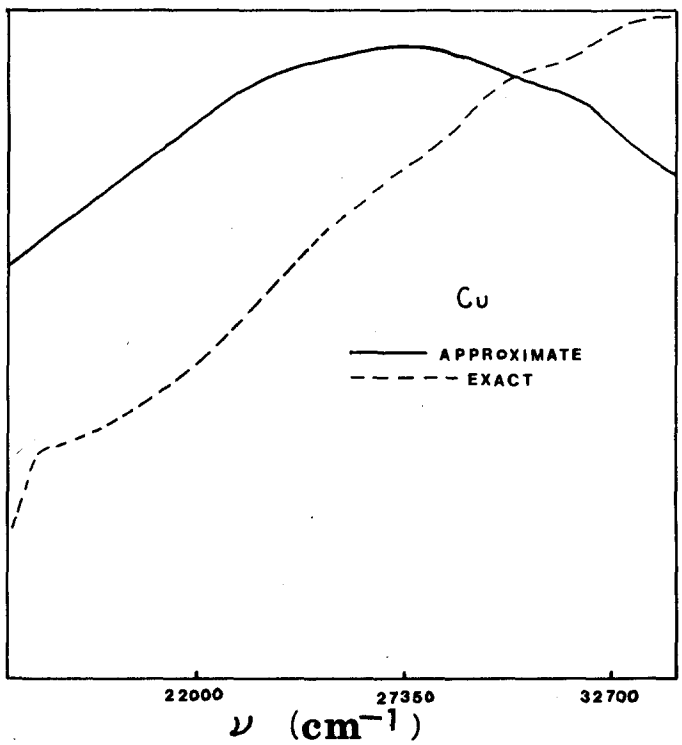

FIG. 2. Comparison of approximate and exact absorption line shapes as a function of wave number for Cu and Ag.

In Table I we present some numerical values for radiative and nonradiative rates associated with Ag, Cu, and Au spheroids. From the above discussion it is clear that the numbers for $\Gamma_{nr}^{(s)}$ presented for Cu should not be taken too seriously. We see that even the relatively long-lived dipolar plasmon in Ag has a lifetime of only about 10^{-14} sec.

In Fig. 3 we plot the ratio of the emission yield of a resonantly excited spheroid divided by the corresponding yield of a sphere of the same volume, as a function of the aspect ratio a/b. This ratio is independent of the dielectric properties of the particle as long as

$$\frac{9}{2}\left(\frac{c}{\omega_1 f}\right)^3 \mathrm{Im}(\epsilon)\,\frac{\xi_0^2-1}{\xi_0}\,[Q_1(\xi_0)]^2 \gg 1\,, \qquad \text{(IV.1)}$$

as may be seen from Eq. (II.7). Since we have assumed that $\lambda \gg f$ in order to neglect retardation effects, this criterion will be met. Thus, the ratio of the yields is simply

$$\frac{Y_{\text{spheroid}}}{Y_{\text{sphere}}} = \frac{1}{9}\left[\frac{\xi_0 Q_1'(\xi_0)}{Q_1(\xi_0)} - 1\right]^2 . \qquad \text{(IV.2)}$$

We see that this ratio grows rapidly with changing aspect ratio. This has to do with the fact that sharp objects (i.e., objects with the high a/b ratios) become good radiators, as they are able to develop sizeable dipoles [see Eq. (I.22)]. The nonradiative rate, however, is not terribly sensitive to the shape factor [see Eq. (II.6)], its variation coming about due to the shift of the resonance frequency and the associated change in the real and imaginary parts of the dielectric constant.

In Fig. 4 a plot of the absorption cross section versus photon energy is given for silver spheroids of fixed volume and various aspect ratios. The volume is taken to correspond to that of a 200 Å radius sphere. The absorption cross section is given by Eq. (II.8). We note that each curve is characterized by a sharp resonance at the plasmon frequency and corresponds to $\hbar\omega = 2.6$, 3.0, and 3.5 eV for $a/b = 3$, 2, and 1, respectively. We note that the plasmon resonance shifts towards lower energies, as the aspect ratio of the spheroid increases, as is expected. The absorption cross section is seen to be rather large on resonance, with typical magnitudes of $10^7 a_0^2$. The cross section at resonance is stronger for sharply peaked structures (larger aspect ratios) than for spherically shaped ob-

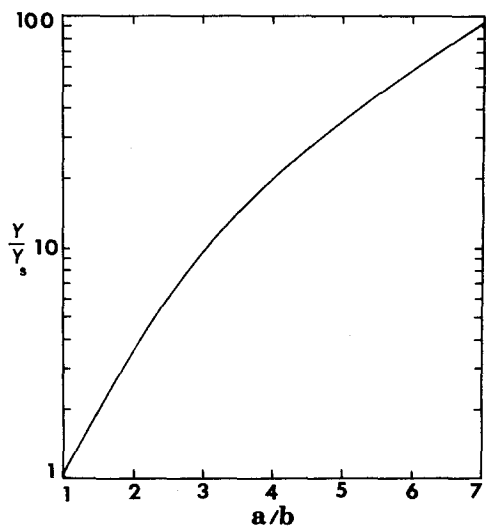

FIG. 3. Yield for a spheroid divided by the yield for a sphere as a function of the aspect ratio of the spheroid a/b.

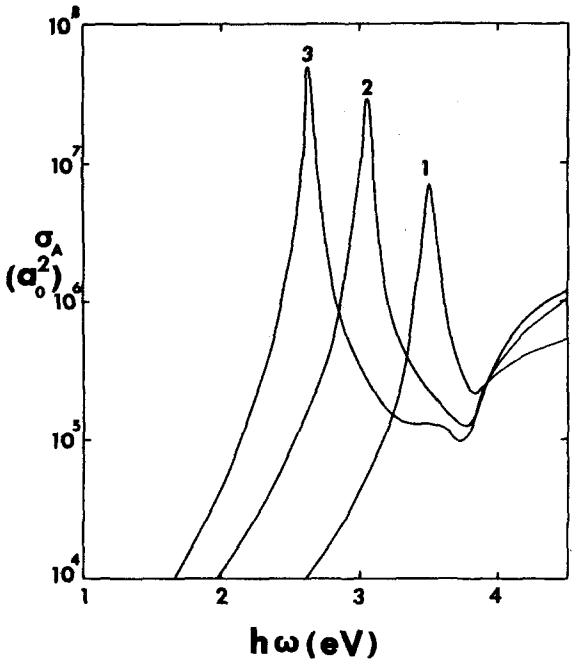

FIG. 4. Absorption cross section, in units of a_0^2, as a function of photon energy $\hbar\omega$ for three silver spheroids of aspect ratios $a/b = 1$, 2, and 3.

jects. This behavior is expected from the functional form of Eq. (II.8) and is a manifestation of the lightning rod effect—a concentration of electric field strength in and around a sharp object, which imples a strong Ohmic heating effect for such an object.

In Fig. 5 the generalized (frequency dependent) yield is plotted as a function of photon energy for silver spheroids that are not resonant with the incident photon. In this case the yield is independent of the aspect ratio but does depend on the volume. Curves (A), (B), and (C) are for columes equal to that of a sphere of radius 500, 200, and 100 Å, respectively. The structure that appears is due to the optical properties of Ag. The basic trend is that larger objects have larger yields. This trend is consistent with the inequality of Eq. (II.3) which holds for an arbitrary shape. It reflects the fact that while the nonradiative power dissipation is proportional to the volume of the particle, the radiative power is proportional to its square. This causes a rise of yield with increasing volume according to Eq. (II.4).

Let us now turn our attention to the case of a molecule near a spheroid. The calculations are performed for a silver particle with a typical organic dye molecule characterized by a resonant frequency $\omega_0 = 25\,600$

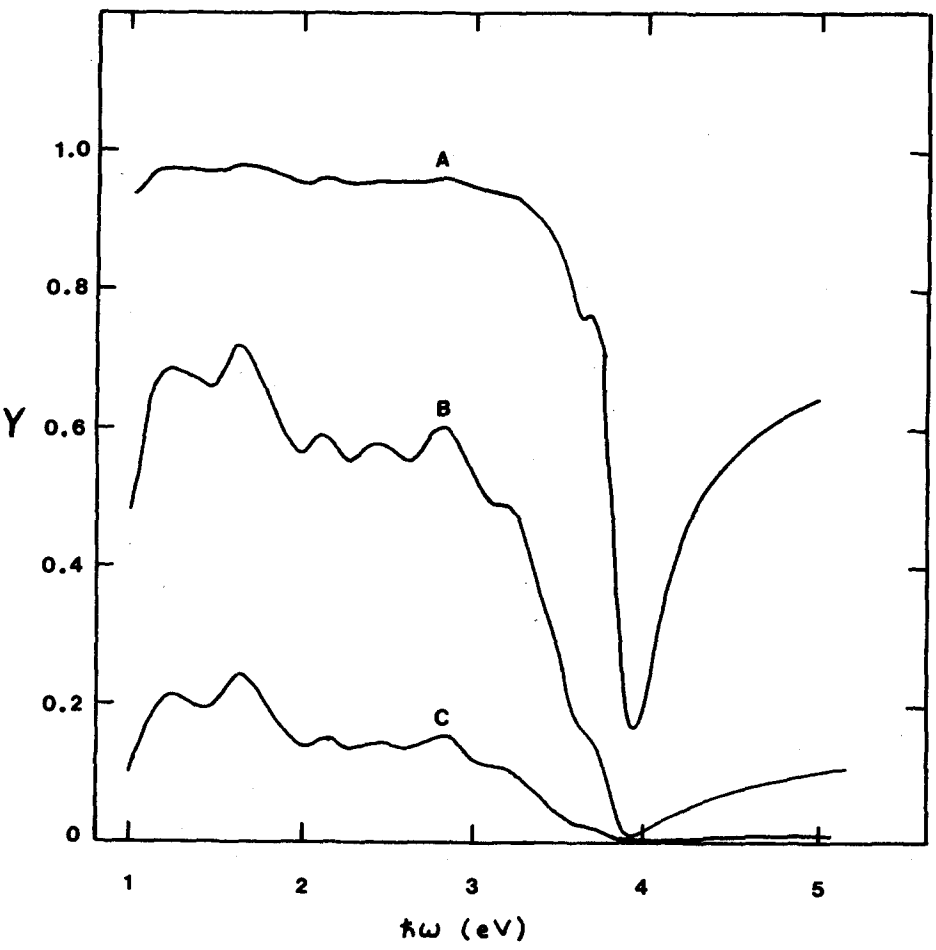

FIG. 5. Yields for silver spheroids as a function of photon energy $\hbar\omega$. Graphs (A), (B), and (C) correspond to particles whose volumes correspond to spheres of 500, 200, and 100 Å radius, respectively.

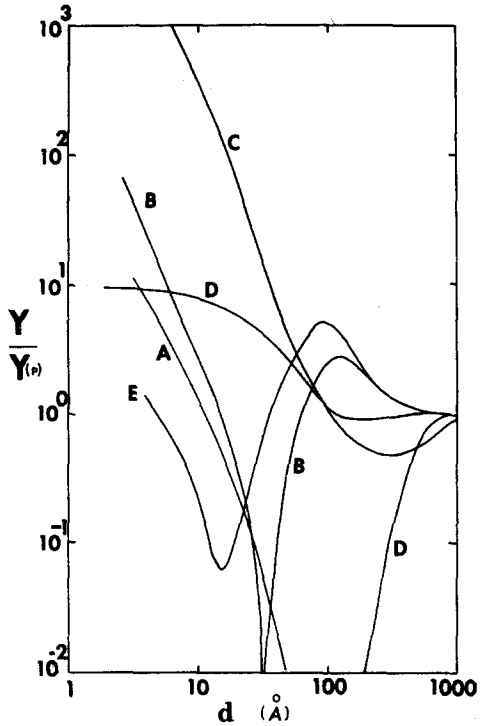

FIG. 6. Ratio of yield for a molecule near a spheroid to a molecule near a plane as a function of molecule–solid distance d. Curve (A) corresponds to a silver sphere with a normal ($\perp$) dipole. Curves (B) and (C) correspond to a resonant spheroid with $a/b = 1.75$ for parallel ($\parallel$) and normal ($\perp$) dipoles. Curves (D) and (E) correspond to a nonresonant spheroid with $a/b = 3.00$ for normal ($\perp$) and parallel ($\parallel$) dipoles

cm^{-1} (3.17 eV), a radiative decay rate $\Gamma_r^f = 4.3 \times 10^8$ Hz, and a quantum yield of unity. In Fig. 6 we plot the yield of the system divided by the corresponding yield that would be obtained if the spheroid were replaced by a plane. This ratio is plotted as a function of molecule–spheroid separation (along the direction of the major axis). This corresponds to a transition moment of $\mu = 7.102 e a_0$. The volume of the spheroid is taken to be equal to that of a sphere with a radius of 200 Å. As mentioned earlier, the resonant frequency of a spheroid changes as the shape parameter (aspect ratio) is varied. A silver sphere has its resonant frequency [corresponding to $\mathrm{Re}(\epsilon) = -2$] at $\hbar\omega = 3.5$ eV. For the above molecular resonance frequency the spheroid has a similar resonance frequency when $a/b = 1.75$. At this frequency $\epsilon = -3.93 + i.192$, so the particle has a relatively small absorptivity. Some characteristic numbers for the radiative and nonradiative decay rates of the model molecule at a distance of 8 Å from the particle surface are given in Table I. In Fig. 6 we present results where the dipole is either perpendicular ($\perp$) or parallel ($\parallel$) to the surface. Curve (A) is for a sphere with the dipole perpendicular to the surface. At small or large molecule–surface separations the yields of the particle near a sphere or a plane are comparable. At intermediate separations (~100 Å) the sphere has a much lower yield. This may be seen by examining Eq. (II.9) for the radiative decay rate, where the possibility for destructive interference between the molecular dipole and the spheroid's dipole can yield a small argument whose absolute square is to be taken. Curves (B) and (C) illustrate the emission yield ratio in the case of a resonant spheroid ($a/b = 1.75$) in the parallel and perpendicular configurations, respectively.

In curve (C) we see that for the same aspect ratio ($a/b = 1.75$) the perpendicular configuration yield ratio is on the order of magnitudes larger than for a sphere. The destructive interference still takes place but now the yield ratio at small d is more than an order of magnitude larger than for a sphere. This is due to the high efficiency for radiating for a sharp object (which exceeds the increased efficiency for nonradiative decay). Finally, curves (D) and (E) are for a nonresonant spheroid ($a/b = 3$) in the $\perp$ and $\parallel$ configurations, respectively. In the case of curve (E) we see evidence for both constructive and destructive interference of the dipoles.

In Fig. 7 the ratio of the radiative decay rates for a molecule near a spheroid $\Gamma_{r,s}$ to a molecule near a plane $\Gamma_{r,p}$ is given. Here the dipole is perpendicular to the particle. In curve (A) the particle is a sphere, in curve (B) it has an aspect ratio 1.75, and in curve (C) it has an aspect ratio 3.0. The enhanced radiative decay at resonance is again evident. In the case of curve (A), the sphere resonance ($\epsilon = -2$) and plane resonance ($\epsilon = -1$) are now sufficiently close that the destructive interference effect is not very strong (although it was stronger in the case of Fig. 6, where the nonradiative decay rates also played a role).

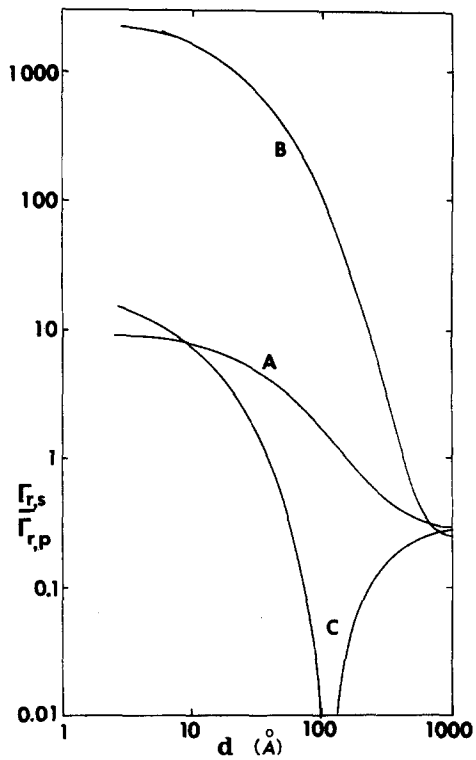

FIG. 7. Ratio of the radiative decay rate for a molecule near a spheroid to the corresponding rate for a molecule near a plane as a function of the molecule–solid distance d. Curve (A) is for a sphere, curve (B) is for a resonant spheroid, with $a/b = 1.75$, and curve (C) is for a nonresonant spheroid, with $a/b = 3.00$.

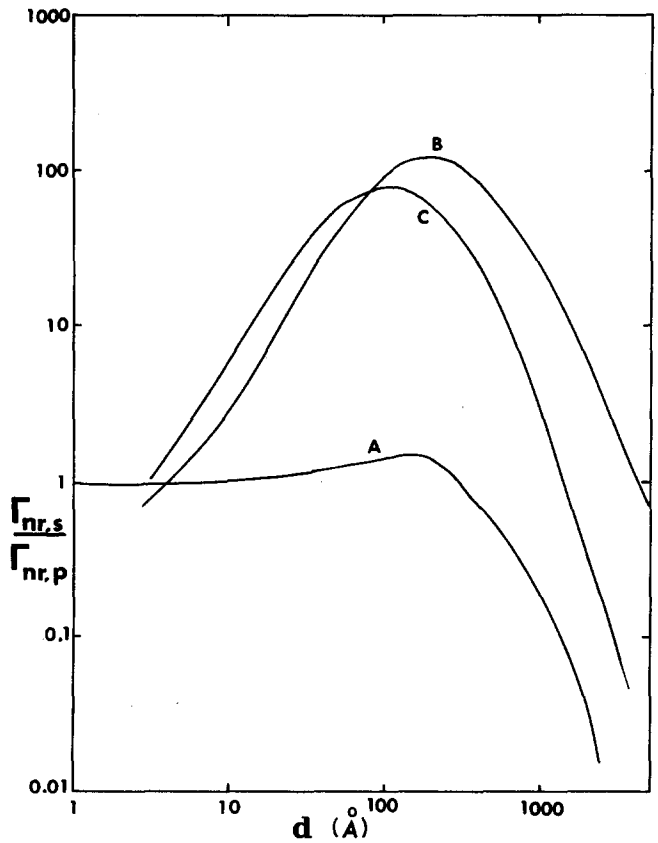

FIG. 8. Ratio of the nonradiative decay rate for a molecule near a spheroid to that of a molecule near a plane as a function of the molecule–solid distance d. The labels are the same as in Fig. 5.

Figure 8 displays the corresponding ratios of the nonradiative decay rates for a molecule near a spheroid $\Gamma_{nr,s}$ to that of a molecule near a plane $\Gamma_{nr,p}$ as a function of molecule–solid separation. Again we restrict our attention to the perpendicular configuration. Curve (A) is for a sphere, curve (B) is for $a/b = 1.75$, and curve (C) is for $a/b = 3$. We note that in the case of a sphere the radiationless decay rate is comparable to that on a plane for distances out to several hundred Å and then the sphere rate falls down relative to the plane rate. For the spheroids, however, there is a peak of two orders of magnitude in the ratio before the falloff sets in. The peak is due to the lightning rod effect. At separations much smaller than the scale which determines the particle shape, this shape does not appreciably affect the Ohmic heating. At intermediate distances, however, a sharp curvature of the surface acts to concentrate the electric field lines, thereby enhancing the Ohmic heating. At large separations (few$\times 10^3$ Å) the plane simply presents more solid to the confronting molecule than does the finite spheroid, and the ratio falls off again.

In Fig. 9 the absolute yield for a molecule near a spheroid is given for the perpendicular configuration. Curve (A) is for a sphere, curve (B) is for an aspect ratio of 1.75, and curve (C) is for $a/b = 3.0$. The resonant enhancement of the yield for $a/b = 1.75$ is apparent.

In Fig. 10 we present the total decay rate as a function of d for a molecule near a silver sphere (A), near a resonant spheroid (B), and near a nonresonant spheroid (C) for a normal configuration. In all cases the decay is

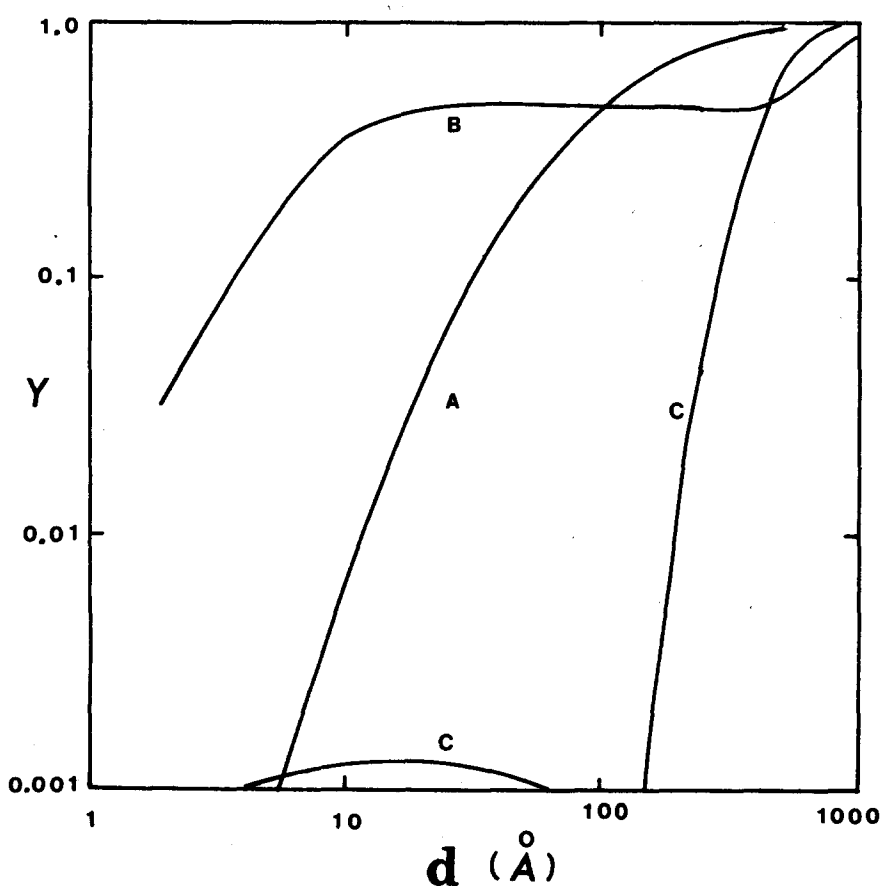

FIG. 9. Yield for a molecule near a silver spheroid as a function of the molecule–spheroid separation d. Curve (A) is for a sphere, curve (B) is for a resonant spheroid with $a/b = 1.75$, and curve (C) is for a nonresonant spheroid with $a/b = 3.0$.

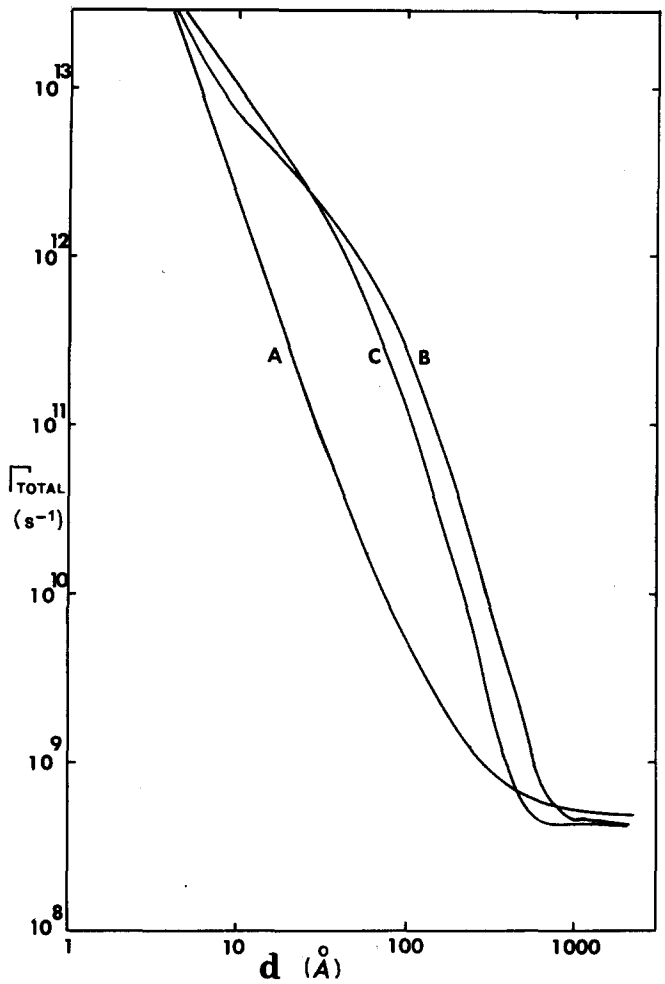

FIG. 10. The total decay rate for a molecule with its dipole perpendicular to the Ag spheroid as a function of molecule–spheroid separation. Curve (A) is for $a/b = 1.0$, (B) is for $a/b = 1.75$ (resonant), and (C) is for $a/b = 3.0$.

seen to fall off rapidly with distance. In the case of spheroids we see that a two order of magnitude increase in the total decay is possible at intermediate separations (30–300 Å). This may be attributed to both a lightning rod effect, as in curve (C), and a plasma resonance effect, as is curve (B). At small distances the total decay is dominated by the nonradiative decay while at large distances it is the radiative decay that dominates. The dip in the total decay rate for the sphere case (A) is traced to the destructive interference in the radiative rate between spheroid and molecule emission.

Let us try to understand the qualitative differences that exist between the case of a molecule near a spheroid and the case of a molecule near a plane. First consider the nonradiative decay. There are two competing effects present. For a fixed distance between the molecule and the object, the molecule "sees" more of the plane than the spheroid. (We could always imagine carving out a spheroidal shape from the half-space behind the surface plane.) This would favor dominance of the nonradiative decay for a plane over that of a spheroid. Such behavior is observed at large separations. Another effect which must be considered, however, is the tendency for a sharp feature of the surface to concentrate electric field lines (the lightning rod effect). This effect is most pronounced when the source (the molecular dipole) is close to the apex of the spheroid. It causes the spheroidal case to dominate over the planar case when the molecule is close to the surface, as far as nonradiative decay is concerned.

In the case of radiative decay one knows that the system dipole remains finite as the molecule approaches a plane. The system dipole consists of the molecular dipole and the image dipole—which is independent of molecule–surface separation. On the other hand, the system dipole for a molecule near a spheroid grows rather intense due to the large amount of charge separation that occurs in the spheroid.

Finally, let's turn our attention to the quantum yield for a molecule near a sphere. In Fig. 11 we plot the ratio of the real quantum yield Y and apparent quantum yield Y_{app} as a function of radius for a silver sphere. The molecule is held fixed at a distance of 16 Å from the surface of the sphere. In these calculations we assume that nonradiative processes can quench the excited state of the molecule even for the molecule far from the surface. The "free" quantum yield is taken to be $Y^{(f)} = 0.005$. For comparison's sake we plot $Y/Y^{(f)}$ as curve (A) and $Y_{app}/Y^{(f)}_{app}$ as curve (B). In these calculations we expect the small sphere theory to break down when the size of the sphere exceeds $\sim \lambda/20 \sim 250$ Å. For larger sphere sizes one expects a reduction of the above yield ratios. Indeed, in the limit of a molecule near a plane one expects Y and Y_{app} to be less than $Y^{(f)}$. The expected behavior is indicated by dashed lines in

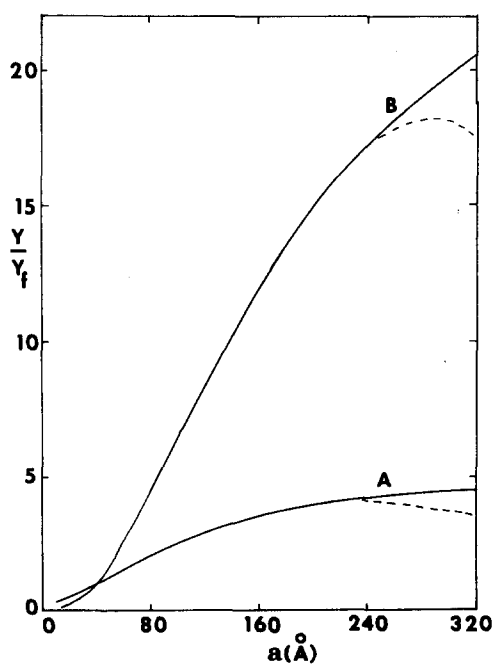

FIG. 11. Ratio of real yield to "free" molecule yield [$Y/Y^{(f)}$, curve (A)] and apparent yield to free molecule yield [$Y_{app}/Y^{(f)}_{app}$, curve (B)], as a function of sphere radius a. The molecule is held fixed at $d = 16$ Å from the surface. The dashed curves indicate the expected large sphere theory behavior.

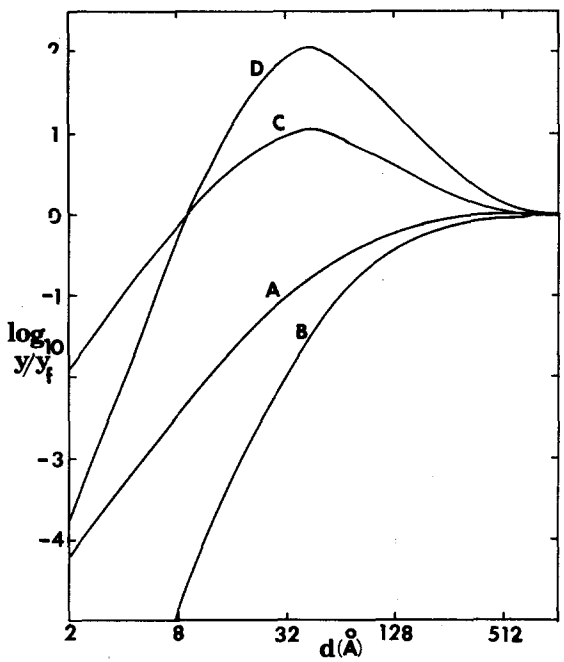

FIG. 12. Yield ratios as in Fig. 11, but plotted as a function of molecule–surface distance d. Curves (A) and (B) are $Y/Y^{(f)}$ and $Y_{app}/Y_{app}^{(f)}$ for $Y^{(f)}=1$, respectively; curves (C) and (D) are $Y/Y^{(f)}$ and $Y_{app}/Y_{app}^{(f)}$ for $Y^{(f)}=0.005$, respectively. The sphere is taken to be fixed in radius at 200 Å and is made of silver.

Fig. 11. Such a behavior has in fact been observed by Glass *et al.*[8(a)] (It should be noted that the observations reported by these authors correspond to Y_{app} rather than Y.)

In Fig. 12 a plot is made of the real and apparent yield ratios $Y/Y^{(f)}$ and $Y_{app}/Y_{app}^{(f)}$ versus distance of the molecule from the sphere d. The sphere size is held fixed at $a=200$ Å. Two cases are shown for each ratio. In one case [(A), (B)] we take the free yield to be unity and plot $Y/Y^{(f)}$ [labeled (A)] and $Y_{app}/Y_{app}^{(f)}$ [label (B)]. In the second case [(C), (D)] we chose $Y^{(f)}=0.005$ and plot $Y/Y^{(f)}$ [labeled (C)] and $Y_{app}/Y_{app}^{(f)}$ [labeled (D)]. We see that the yield ratios are dependent on the size of $Y^{(f)}$.

V. CONCLUSIONS

We have studied the radiative and nonradiative lifetimes and the corresponding emission yields associated with small dielectric spheroidal grains and with molecules located outside and inside such grains. We have limited ourselves to distances and dimensions much smaller than the radiation wavelength whereupon retardation effects were neglected. We have seen that the radiationless and radiative lifetimes of a molecule interacting with such dielectric particles are substantially different than those of free molecules or of molecules placed near plane surfaces.

Our models are relevant to small dielectric particles formed in dilute colloidal solutions or in island films embedded in solid matrices or generated in supersonic beams. In addition, these models contain part of the physics which underlies the behavior of rough dielectric surfaces and of molecules adsorbed on such a surface. Missing are the effect of the underlying dielectric bulk and the effect of interactions between dielectric particles (the latter should be taken into account also in treatments of the small particle systems listed above, at higher particle concentrations). These effects will be studied in future work. Another related problem of interest concerns the possibility of observing superradiant emission from a distribution of molecules embedded in such grains. A grain containing many excited molecules constitutes an excited system whose dimensions are smaller than the radiation wavelength for which the superradiance effect was predicted.[22] However, the occurrence of superradiance depends on the competition between the emission and between internal dephasing effects. The recent observation by Fork and Taylor[23] of unexpectedly short radiative lifetimes in grains of some Eu^{3+} salts may be related to this phenomenon.

The peculiar optical behavior of small dielectric particles has been recently a subject of intensive research effort. We see that special effects are encountered only for molecules interacting with such particles. Experiments pertaining to the optical behavior of such molecules and of molecules adsorbed on rough surfaces are highly desirable.

ACKNOWLEDGMENTS

A. N. thanks the U.S.–Israel Binational Science Foundation for partial support of this work. J. G. thanks the C. U. N. Y. P. S. C.–B. H. E. research award program for partial support of this work. We thank D. Weitz, S. Garoff, and L. E. Brus for helpful discussions.

[1]For general review articles on SERS see (a) R. P. Van Duyne in *Chemical and Biochemical Applications of Lasers*, edited by C. B. Moore (Academic, New York, 1978), Vol. 4; (b) E. Burstein, C. Y. Chen, and S. Lindquist, in *Proceedings of the* US–USSR *Symposium on the Theory of Light Scattering in Condensed Matter* (Plenum, New York, 1979); (c) T. E. Furtak and J. Reyes, Surf. Sci. **93**, 351 (1980); (d) S. Efrima and H. Metiu, Israel J. Chem. **17**, 18 (1979).

[2]For experimental indication of the relation between SERS and the modified local electromagnetic field see (a) M. Moskovitz, J. Chem. Phys. **69**, 4159 (1978); Solid State Commun. **32**, 59 (1979); (b) J. A. Creighton, C. G. Blatchford, and M. G. Albrecht, J. Chem. Soc. Faraday Trans. **75**, 790 (1979); (c) J. G. Bergman, D. S. Chemla, P. F. Liao, A. M. Glass, A. Pinczak, R. M. Hart, and D. H. Olson, "On the relationship Between Surface Enhanced Raman Scattering and Dielectric Properties of Aggregated Silver Films (to be published); (d) P. F. Liao, J. G. Bergman, D. S. Chemla, A. Wokaun, J. Melngailis, A. M. Hawryluk, and N. P. Economou, "Surface Enhanced Raman Scattering from Microlithographic Silver Particles" (to be published); (e) D. A. Zwemer, C. V. Shank, and J. E. Rowe, Chem. Phys. Lett. **73**, 201 (1980); (f) D. A. Weitz, T. J. Gramila, A. Z. Genack, and J. I. Gersten, Phys. Rev. Lett. **45**, 355 (1980); (g) A. Girlando, M. R. Philpott, D. Heitmann, J. D. Swalen, and R. Santo, J. Chem. Phys. **72**, 5187 (1980); (h) P. N. Sanda, J. M. Warlaumont, J. E. Demuth, J. C. Tsang, K. Christmann, and J. A. Bradley, Phys. Rev. Lett. **45**, 1519 (1980); J. C. Tsang, J. R. Kirtley, and T. N. Theis, Solid State Commun. **35**, 667 (1980); J. C. Tsang, J. R. Kirtley, and J. A. Bradley, Phys. Rev. Lett. **43**, 772 (1980).

[3]For theoretical models which lead to enhanced local field see Ref. 2(a) and (a) F. W. King, R. P. Van Duyne, and G. C. Schatz, J. Chem. Phys. **69**, 4472 (1978); (b) S. Efrima and H. Metiu, J. Chem. Phys. **70**, 1602 (1979); (c) C. Y. Chen and E. Burstein, Phys. Rev. Lett. **45**, 1287 (1980); (d) M. Kerker, D. S. Wang, and H. Chew, Appl. Opt. **19**, 2256 (1980) and to be published; (e) S. L. McCall, P. M. Platzman, and P. A. Wolff, Phys. Lett. A **77**, 381 (1980); (f) S. S. Jha, J. R. Kirtley, and J. C. Tsang, Phys. Rev. B **22**, 3973 (1980); (g) J. I. Gersten, J. Chem. Phys. **72**, 5779 (1980); (h) J. I. Gersten and A. Nitzan, J. Chem. Phys. **73**, 3023 (1980).

[4]J. C. Tsang and J. Kirtley, Solid State Commun. **30**, 617 (1979); E. Burstein and C. Y. Chen, Proceedings of the VIIth International Conference on Raman Spectroscopy, Ottawa, 1980.

[5]M. Kerker, O. Siiman, L. A. Bumm, and D. S. Wang, Appl. Opt. (in press); A. Abe, W. Schulze, K. Manzel, and M. Moskovitz, "Surface Enhanced Raman Spectroscopy of CO Adsorbed on Colloidal Silver Particles" (to be published).

[6](a) P. R. Hilton and D. W. Oxtoby, J. Chem. Phys. **72**, 6346 (1980); (b) G. Korzeniewski, T. Maniv, and H. Metiu, Chem. Phys. Lett. **73**, 212 (1980); (c) P. J. Feibelman, Phys. Rev. B **22**, 3654 (1980).

[7]A. Harstein, J. R. Kirtley, and J. C. Tsang, Phys. Rev. Lett. **45**, 301 (1980).

[8](a) A. M. Glass, P. F. Liao, J. G. Bergman, and D. H. Olson, Opt. Lett. **5**, 368 (1980); (b) G. Ritchie, C. Y. Chen, and E. Burstein, Reported in the 7th International Conference on Raman Spectroscopy, Ottawa, 1980.

[9]A. Nitzan and L. E. Brus (to be published).

[10]For a review see R. R. Chance, A. Prock, and R. Silbey, Adv. Chem. Phys. **37**, 1 (1978).

[11]A. Sommerfeld, *Partial Differential Equations in Physics* (Academic, New York, 1949), Chap. 6.

[12]B. van der Pol and H. Bremmer, Philos. Mag. **24**, 141; 824 (1937); **25**, 817 (1938).

[13]Since we limit ourselves to dimensions much smaller than the radiation wavelength, we do not have to use the general results of Ref. 12.

[14](a) B. Mie, Ann. Phys. (Leipzig) **25**, 377 (1908); for modern reviews see (b) M. Born and E. Wolf, *Principles of Optics* (Pergamon, Oxford, 1975), 5th edition; (c) J. D. Jackson, *Classical Electrodynamics* (Wiley, New York, 1975); (d) M. Kerker, *The Scattering of Light and Other Electromagnetic Radiation* (Academic, New York, 1969).

[15]H. Chew, P. J. McNulty, and M. Kerker, Phys. Rev. A **13**, 396 (1976); M. Kerker, P. J. McNulty, M. Sculley, H. Chew, and D. D. Cook, J. Opt. Soc. Am. **68**, 1675; 1686 (1978); P. J. McNulty, S. D. Druger, M. Kerker, and H. W. Chew, Appl. Opt. **18**, 1484 (1979); H. Chew, D. D. Cooke, and M. Kerker, Appl. Opt. **19**, 44 (1980).

[16]R. Rosetti and L. E. Brus, J. Chem. Phys. **73**, 572 (1980).

[17]The sphere case has been solved by Mie[14(a)] without the restrictions to dimensions much smaller than λ. Small spheroids were also considered.[14(d)] The present approach is different than those taken before and provides an example to the route taken later in the presence of a dipole. Furthermore, we evaluate the radiative and nonradiative lifetimes of the spheroid plasmons which were not obtained in former work.

[18]The equivalent problem of a molecule within a dielectric particle has been studies by Kerker and co-workers[13] for a general size sphere and for a cylinder.

[19]In Mie's theory and in the present paper the term absorption cross section is used to describe the nonradiative dissipation of the incident radiation energy. The cross section for removal of intensity from the incident beam $\sigma_{ex}=\sigma_a+\sigma_r$ is called the extinction cross section. In molecular spectroscopy the term absorption cross section is usually used for σ_{ex}.

[20]The transformation into a Wigner–Breit form with frequency independent Γ_{nr} is valid only provided that $|\partial\epsilon_2(\omega_1)/\partial\omega_1| \ll |\partial\epsilon_1(\omega_1)/\partial\omega_1|$, where $\epsilon_1=\mathrm{Re}\epsilon$, $\epsilon_2=\mathrm{Im}\epsilon$. When this inequality holds we can also write $\Gamma_{nr}=2\epsilon_2(\omega_1)/[\partial\epsilon_1(\omega_1)/\partial\omega_1]$.

[21]It can be shown that if $d=R-a\ll a$, the total surface damping rate is dominated by the $l>1$ modes so that $\Gamma'_{nr,s}\simeq\Gamma_{nr,s}$ ($\Gamma_{nr,s}$ is calculated in Sec. II).

[22]R. H. Dicke, Phys. Rev. **93**, 99 (1954).

[23]R. L. Fork and D. W. Taylor, Phys. Rev. B **19**, 3365 (1979).

[24]A copy of the mathematical appendices to this paper has been deposited with the Physics Auxiliary Publication Service, see AIP document no. PAPS JCPSA-75-1139-32 for 32 pages of these appendices. Order by PAPS number and journal reference from American Institute of Physics, Physics Auxiliary Publication Service, 335 East 45th Street, New York, N. Y. 10017. The price is $1.50 for each microfiche (98 pages), or $5 for photocopies of up to 30 pages with $0.15 for each additional page over 30 pages. Airmail additional. Make checks payable to the American Institute of Physics.